American Mineralogist, Volume 69, pages 200–206, 1984

Santaclaraite, a new calcium-manganese silicate hydrate from California

RICHARD C. ERD

U.S. Geological Survey, Menlo Park, California 94025

AND YOSHIKAZU OHASHI

Department of Geology, University of Pennsylvania
Philadelphia, Pennsylvania 19104

Abstract

Santaclaraite, ideally $CaMn_4[Si_5O_{14}(OH)](OH) \cdot H_2O$, occurs as pink and tan veins and masses in Franciscan chert in the Diablo Range, Santa Clara and Stanislaus Counties, Calif. It is associated with four unidentified Mn silicates, Mn-howieite, quartz, braunite, calcite, rhodochrosite, kutnohorite, barite, harmotome, chalcopyrite, and native copper. Santaclaraite is triclinic, space group $B\bar{1}$, a = 15.633(1), b = 7.603(1), c = 12.003(1)Å, α = 109.71(1)°, β = 88.61(1)°, γ = 99.95(1)°, V = 1322.0(3)Å^3, Z = 4. The strongest lines of the X-ray powder pattern are (d, I, hkl): 7.04Å, 100, 010; 3.003, 84, $\bar{5}01$; 3.152, 80, 410; 7.69, 63, 200; 3.847, 57, ($1\bar{1}3$,400); 3.524, 39, 020. Crystals are lamellar to prismatic (flattened on {100}), with good cleavage on {100} and {010}; H = 6½; D(calc.) = 3.398 g/cm^3, D(meas.) = 3.31(±0.01); optically biaxial negative, with α = 1.681, β = 1.696, γ = 1.708 (all ±0.002), $2V_X$ = 83 (±1)°. Although chemically a hydrated rhodonite, santaclaraite dehydrates to Mn-bustamite at about 550°C (in air). Santaclaraite is a five-tetrahedral-repeat single-chain silicate and has structural affinities with rhodonite, nambulite, marsturite, babingtonite, and inesite.

Introduction

The new mineral santaclaraite was discovered in 1975 in an abandoned manganese mine in the Diablo Range in northeastern Santa Clara County, Calif., by Messrs. John L. Parnau and Albert L. McGuinness, who brought it to us for investigation. They suspected that the mineral was inesite from its color and prismatic habit, but our studies proved the mineral to be new and to have a crystal structure that helps to clarify the role of hydrogen in pyroxenoids (Ohashi and Finger, 1981). The mineral is named for the County of Santa Clara, the locality of its first occurrence. Specimens of santaclaraite (holotype and cotypes) will be deposited at the Smithsonian Institution (National Museum of Natural History), Washington, D.C. The name and description have been approved by the Commission on New Minerals and Mineral Names, I.M.A. A description given by Ohashi and Erd (1978) of an unnamed new mineral was a preliminary report for santaclaraite.

Occurrence and paragenesis

Although the discoverers of santaclaraite did not disclose the exact location of its occurrence, they have provided us with many specimens from the locality and partial information on the occurrence. The mine is one of about fifty abandoned manganese mines located in Santa Clara, Alameda, San Joaquin, and Stanislaus Counties near their common junction. Nearly all these mines lie within a circle of 16-km radius centered on Mount Boardman at this junction. The mines and the geology of the area were described by Jenkins (1943) and Trask (1950), and a review with later production figures was presented by Davis (1957). The manganese ore bodies in the four-county area are of the Coast Range sedimentary type that occur in chert of the Franciscan Complex (Jurassic to Lower Tertiary).

Our present information from the discoverers is that the abandoned mine in which santaclaraite was discovered is on property that is now private, posted against trespassing, and patrolled by a security system. The mine workings are no longer accessible, and all of the manganese mineral specimens were found on old dumps at this site.

The paragenesis of the specimens that we have seen from this locality is noteworthy in that the more common Mn minerals are scarce or absent and the Mn silicates so far found are all unusual in some respects. It seems worthwhile, therefore, to give a detailed account of the associated Mn minerals. Santaclaraite occurs both as cross-fiber veins (the largest measures 1 cm in width by more than 9 cm in length) and irregular masses (10 cm in

0003–004X/84/0102–0200$02.00

maximum dimension) in Mn-oxide-stained chert and quartz. Though uncommon in its overall occurrence, santaclaraite is the most abundant Mn silicate at this locality. The next most abundant Mn silicate is an unidentified reddish-brown fine-grained mineral that appears to be a member of the friedelite series. Three other unidentified Mn silicates at this locality are similar to, but differ in some respects from, the minerals parsettensite, welinite, and gageite (all currently under study). Mn-howieite is associated with santaclaraite as yellow-brown fibrous veinlets, masses, and small spherules, with $\alpha = 1.697$, $\beta = 1.716$, $\gamma = 1.727$ (all ± 0.002). Fine-grained rhodochrosite is subordinate to the Mn silicates but is widely disseminated throughout them and the quartz matrix. Calcian kutnohorite and calcian rhodochrosite were found in a single occurrence as small scalenohedra (to 0.6 mm). The central cores of the crystals consist of massive white Ca-kutnohorite ($a = 4.919$, $c = 16.525$Å; $\omega = 1.702$, $\varepsilon = 1.518$, both ± 0.002) encrusted with tiny euhedral rhombs of Ca-rhodochrosite ($a = 4.824$, $c = 16.01$Å; $\omega = 1.785 \pm 0.003$, $\varepsilon = 1.518 \pm 0.002$). A strong positive microchemical test was obtained for Mn, but Fe could not be detected. The data indicate about 20 mole percent $CaCO_3$ in the rhodochrosite, which is near the limit for naturally occurring material (Deer *et al.*, 1962, p. 265–267). All the specimens that we have seen are stained black with a thin coating of X-ray amorphous Mn oxide, although very little of this material is actually present. The Mn mineral that was mined at this locality appears to have been braunite, which occurs as masses and veins, up to 6 cm across in the specimens that we have seen. Other associated minerals are calcite (some manganoan), barite, and rare harmotome, chalcopyrite, and native copper. Some of the quartz is colored dark grayish blue by inclusions of asbestiform riebeckite.

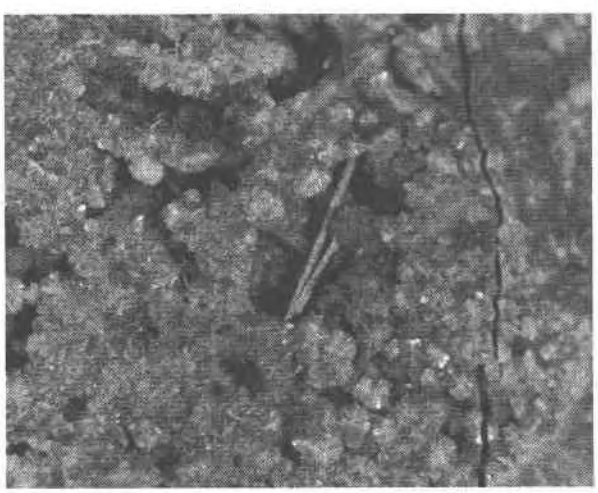

Fig. 1. Vuggy radiated pink santaclaraite, with prismatic crystals of tan santaclaraite (larger is 7.5 mm long) projecting into vug at center. Photograph by Lowell Kohnitz, U.S. Geological Survey.

A second occurrence of santaclaraite was discovered at the Buckeye mine (located in sections 2 and 3, T. 5 S., R. 5 E., in Stanislaus County, Calif.). The mineral was identified by Erd in specimens collected in 1942–1944 from the ore body by Dr. Max D. Crittenden, Jr., during his study of the geology of the deposit (Trask, 1950, p. 287–289). Santaclaraite occurs sparsely as pink prismatic crystals up to 3 mm long in quartz veins in tan chert associated with rhodochrosite, the friedelite-like mineral (identical with that of the Santa Clara Co. occurrence), braunite, and very minor chalcopyrite. It is probable that at least some of the "inesite" identified in the mine by Crittenden is actually santaclaraite (Crittenden, oral communication, 1980). The underground workings at the abandoned Buckeye mine are no longer accessible and an attempt to find santaclaraite in the present-day (1981) dumps was unsuccessful.

Crystallography

Morphology

Santaclaraite occurs principally as radiated lamellar aggregates (Fig. 1) composed of thin prismatic to tabular subhedral crystals, flattened on {100}. The rough spherules average about a millimeter in diameter. Where space permits, thick prismatic euhedra, up to a centimeter in length on [001], are developed; several of these are visible in the vug in Figure 1. The mineral also occurs in cross-fiber veins composed of prismatic to nearly fibrous crystals having a length/width ratio up to 40. Forms identified with a two-circle optical goniometer are *b* {010}, *a* {100} the most prominent form, *m* {110}, *f* {101}, *g* {301}, and *h* {401}. Simple twinning on {100} is common.

X-ray data

The preliminary unit-cell dimensions of santaclaraite were determined from single-crystal X-ray precession photographs using Zr-filtered Mo radiation. Table 1 lists these data, refined by least-squares analysis of the X-ray powder data. The crystal structure of santaclaraite has been determined by Ohashi and Finger (1981); the mineral has centric triclinic symmetry ($P\bar{1}$ for the primitive cell). An *I*-centered cell was employed by Ohashi and Finger for structural comparison of santaclaraite with other pyroxenoids; however, a *B*-centered cell is selected here on the basis of morphology for the mineralogic description. Table 1 compares the data for the various settings.

The X-ray powder data are shown in Table 2. There is a moderately strong preferred orientation of *hk*0 reflections in the X-ray diffractometer pattern due to the good {010} and {100} cleavages. The intensities observed *in powder photographs* agree closely with the calculated intensities and so are not listed in Table 2. The effect of the preferred orientation is most noticeable for the lines at $d = 2.692$ and 2.939Å, which are the strongest in powder photographs.

Table 1. Unit-cell data for santaclaraite

System	Triclinic	Triclinic	Triclinic
Space group	$P\bar{1}$	$B\bar{1}$*	$I\bar{1}$*
a (Å)	9.738(2)**	15.633(1)	10.291(1)
b	9.970(1)	7.603(1)	11.934(2)
c	7.603(1)	12.003(3)	12.003(4)
α	109.77(1)°	109.70(1)°	105.78(1)°
β	93.95(1)°	88.61(1)°	110.65(2)°
γ	104.97(2)°	99.95(1)°	89.09(1)°
V (Å^3)	661.0(1)	1322.0(3)	1322.0(4)
Z	2	4	4
D (g/cm^3)	3.398 (idealized composition) 3.379 (chemical analysis)		
D	3.31(±0.01)†		

* Alternative settings used for mineralogical and crystal structural descriptions. Cell transformation matrices are [$-\frac{1}{2}$ 0 $\frac{1}{2}$ / $\frac{1}{2}$ 0 $\frac{1}{2}$ / 010] from the $B\bar{1}$ to $P\bar{1}$ cell and [121/$\bar{1}$21/00$\bar{1}$] from the $B\bar{1}$ to $I\bar{1}$ cell.

** Data obtained from refinement of X-ray powder data (Table 2), using the least-squares program of Appleman and Evans (1973). Parenthesized figures represent the estimated standard deviation (esd) in terms of least units cited for the value to their immediate left, thus 9.738(2) indicates an esd of 0.002.

† Determined in methylene iodide/acetone mixture checked with a Westphal balance.

Physical and optical properties

Santaclaraite is pale pink (Munsell color 5RP 8/2) or moderate reddish orange (10R 6/6). Although these two color varieties are quite distinctive, we observed no significant differences in their chemical composition or optical properties. The color of the pale-pink variety darkens to orange when exposed to tungsten X-radiation. The mineral is transparent and has a vitreous luster and a very pale pink streak. It is nonfluorescent. Cleavage is good on both {100} and {010}. Its hardness is 6½ (Mohs).

Santaclaraite is biaxial negative: $\alpha = 1.681$, $\beta = 1.696$, $\gamma = 1.708$ (all ±0.002; Na light); $2V_X = 83(\pm 1)°$; $r > v$, moderate. The optical orientation is $Z \wedge c = 2°$, $X \wedge b = -21°$ in {100} sections; $Z \wedge c = 16°$, $Y \wedge a = -14.5°$ in {010} sections. Thick sections of santaclaraite show a weak pleochroism, with X = very pale red, Y = pale red, and Z = pale reddish brown; absorption is $Y > Z > X$. The optical properties were determined using a spindle stage with X-ray oriented crystals.

Chemistry

Analyses were made of both pink and tan santaclaraite, using the Geophysical Laboratory MAC electron micro-

Table 2. X-ray powder diffraction data for santaclaraite

Calculated*			Observed**		Calculated			Observed**	
$hk\ell$	$d_{hk\ell}$(Å)	I	I	$d_{hk\ell}$(Å)	$hk\ell$	$d_{hk\ell}$(Å)	I	I	$d_{hk\ell}$(Å)
200	7.694	44	63	7.69	$\bar{3}13$	2.666	19	4	2.666
010	7.048	85	100	7.04	$5\bar{2}1$	2.610	26	20	2.609
$1\bar{1}1$	6.142	11	4	6.15	$\bar{6}10$	2.558	---	6	2.557
210	4.796	33	38	4.797	$1\bar{3}1$	2.512	18	11	2.511
$3\bar{1}1$	4.514	6	4	4.518	$3\bar{3}1$ 420	2.399 2.398	---	8	2.399
$\bar{3}11$	3.967	6	4	3.969					
$1\bar{1}3$ 400	3.849 3.847	24	57	3.847	$\bar{5}21$ $1\bar{1}5$	2.380 2.378	---	2	2.378
$\bar{1}21$	3.791	---	2	3.791	$5\bar{1}3$	2.353	21	5	2.353
$4\bar{1}0$	3.656	---	2	3.652				7	2.743
								7	2.238
$\bar{2}12$	3.598	---	6	3.598					
$0\bar{2}0$	3.524	16	39	3.524				6	2.209
$2\bar{2}2$	3.458	11	5	3.456				38	2.200
$\bar{2}20$	3.438	---	4	3.441				4	2.161
$3\bar{2}1$	3.312	5	5	3.312				11	2.144
								4	2.118
$4\bar{1}2$	3.287	11	5	3.290					
410	3.153	55	80	3.152				5	2.058
$40\bar{2}$	3.126	13	8	3.125				5	2.052
$5\bar{1}1$	3.001							2	2.023
$\bar{5}01$	2.997	88	84	3.003				2	1.920
$0\bar{1}4$	2.993							4	1.872
$\bar{1}13$	2.937	89	13	2.939				6	1.865
$\bar{1}21$	2.930	58	13	2.932				4	1.836
$\bar{3}21$	2.854	8	6	2.853				6	1.787
$32\bar{1}$	2.801	6	4	2.801				6	1.707
$0\bar{2}4$	2.691	100	7	2.692				20	1.682

Plus additional lines all with $I \leq 15$

* All lines are indexed to $d_{hk\ell} \geq 2.350$Å. Indices from least-squares analysis of X-ray powder data, using the digital-computer program of Appleman and Evans (1973). Intensities calculated by a program of Smith and Holomany (1978).

** X-ray diffractometer conditions are: Chart No. X3917; Cu/Ni radiator; $\lambda CuK\alpha_1$=1.540598 Å; silicon used as internal standard; scanned at 1/4° per minute from 4-100° 2θ.

probe with an accelerating voltage of 15 kV and a specimen current of 0.05 μA. The results of the analysis of the tan santaclaraite are shown in Table 3. As noted above, the analysis of the pink material is so similar that it is not reported here. The matrix corrections made are those proposed by Bence and Albee (1968) and programmed by Finger and Hadidiacos (1972) for the microprobe-analysis system. The standards used (Table 3) were selected on the basis of the beta factor in the Bence–Albee method. There is "superior" agreement ($1-K_p/K_c = +0.002$) between the chemical data, optical data, and specific gravity, using the compatibility index of Mandarino (1981) for the Gladstone–Dale relationship.

The formula of santaclaraite, obtained by combining the electron-microprobe analysis data of Table 3 with the crystal-structure data of Ohashi and Finger (1981), is: $(Ca_{0.87}Na_{0.03})(Mn^{2+}_{3.94}Mg_{0.05}Fe^{2+}_{0.01}Ni_{0.01}Co_{0.01})[(Si_{5.04}Al_{0.02})O_{14.03}(OH)_{0.97}](OH) \cdot H_2O$, or, ideally, $CaMn_4[Si_5O_{14}(OH)](OH) \cdot H_2O$. All manganese was assumed as Mn^{2+} in calculating the above formula. This assumption is based on Mn–O bond distances (around 2.2Å) for santaclaraite (Ohashi and Finger, 1981).

Santaclaraite is insoluble or only very slightly soluble in hot concentrated acids. When the mineral is heated in a closed tube, a moderate amount of water is driven off (pH = 5), and the mineral turns light brown; with stronger heating, to about 1000°C, the mineral turns white and nearly opaque.

Related minerals

Santaclaraite is *chemically* a hydrated rhodonite, although *structurally* hydrogen atoms play three different roles (for structural discussion see Ohashi and Finger, 1981). In addition to rhodonite, several minerals are known that are structurally related to santaclaraite (Table 4); these minerals all have silicate chains with five tetrahedral repeats and bands of octahedral cations. Inesite, which is visually very similar to santaclaraite, is a double-chain silicate (Wan and Ghose, 1978): the others are single-chain silicates.

The number of hydrogen atoms (*e.g.*, per five silicons) of santaclaraite is higher than those of babingtonite, nambulite, and marsturite but less than that of inesite. If only chemical formulas are considered, incorporation of hydrogen into an anhydrous formula $M^{2+}{}_5Si_5O_{15}$ or $M^{2+}{}_{10}Si_{10}O_{30}$ can be accomplished by the following changes:

Table 3. Electron-microprobe analysis of santaclaraite

	Wt%		Cations (based on 17 oxygens)		Calc. compn. (wt%) for CaO·4MnO·5SiO$_2$·2H$_2$O
SiO_2	44.74*	Si^{4+}	5.045		44.42
Al_2O_3	0.12	Al^{3+}	0.016	Σ=5.061	
MgO	0.31	Mg^{2+}	0.052		
MnO	41.26	Mn^{2+}	3.941		41.96
FeO	0.09	Fe^{2+}	0.008		
NiO	0.06**	Ni^{2+}	0.005		
CoO	0.06**	Co^{2+}	0.005	Σ=4.011	
CaO	7.24	Ca^{2+}	0.873		8.29
Na_2O	0.12	Na^{1+}	0.026	Σ=0.901	
H_2O	5.28***	H^{1+}	3.972		5.33
Total	99.28				100.00

* Yoshikazu Ohashi, analyst. Standards used: triphylite for Mn; forsterite for Fe; a glass of diopside65-jadeite35 composition for Na, Mg, and Al; wollastonite for Si and Ca; orthoclase for K.

** Determined by Jun Ito (written comm., 1977), using both atomic absorption and spectroscopic methods. Also present are: V_2O_5 <0.01 wt%; Ba, Sr, Ti, and Cr <0.001 wt%.

*** Microcoulometric determination by Marcelyn Cremer (U.S. Geological Survey). Average of two determinations on 46- and 34-mg samples.

Table 4. Chain silicate minerals with five tetrahedral repeats

Mineral name	Idealized chemical formula	Reference to crystal structure
Santaclaraite	$CaMn_4[Si_5O_{14}(OH)](OH)\cdot H_2O$	[1]
Rhodonite	$CaMn_4[Si_5O_{15}]$	[2]
Babingtonite	$Ca_2(Fe^{2+},Mn)Fe^{3+}[Si_5O_{14}(OH)]$	[3]
Nambulite	$(Li,Na)Mn_4[Si_5O_{14}(OH)]$	[4]
Marsturite	$NaCaMn_3[Si_5O_{14}(OH)]$	[5]
Inesite	$Ca_2Mn_7[Si_{10}O_{28}(OH)_2]\cdot 5H_2O$	[6]

[1] Ohashi and Finger (1981).

[2] e.g., Peacor and Niizeki (1963), Ohashi and Finger (1975).

[3] Araki and Zoltai (1972).

[4] Narita et al. (1975), Murakami et al. (1977).

[5] Peacor et al. (1978).

[6] Wan and Ghose (1978).

Table 5. Unit-cell data for Ca-bustamite, Mn-bustamite, and dehydrated santaclaraite

	Ca-bustamite MP-138*	Mn-bustamite MP-101*	Dehydrated Santaclaraite**
$CaSiO_3$ (mol%)	78.8	33.8	24(?)
Space group	$A\bar{1}$	$A\bar{1}$	$A\bar{1}$
a (Å)	7.848(3)	7.639(3)	7.616(2)
b	7.263(5)	7.098(4)	7.090(3)
c	13.968(1)	13.726(2)	13.615(3)
α	90.16(3)°	89.72(3)°	89.94(3)°
β	95.25(2)°	94.82(2)°	94.44(2)°
γ	103.36(3)°	103.07(3)°	103.37(3)°
V (Å^3)	771.1(5)	722.3(4)	713.0(3)
Molar V (cm^3)	38.70	36.25	35.78
D (gcm^{-3})	3.086	3.480	3.560
D (meas.)†	3.082	3.455	---

* Specimens from Broken Hill, N.S.W., Australia, described by Mason (1973). Data obtained from refinement of X-ray powder data (Table 5) using the least-squares program of Appleman and Evans (1973). Error in parentheses is one standard deviation.

** Santaclaraite heated in air at approximately 1,000°C for five hours.

† Data from Mason (1973).

Table 6. X-ray powder diffraction data for Ca-bustamite, Mn-bustamite, and dehydrated santaclaraite

Calculated*			Observed						Calculated**	
			Ca-bustamite MP-18†		Mn-bustamite MP-101††		Dehydrated Santaclaraite†††			
hkℓ	$d_{hk\ell}$(Å)	I	$d_{hk\ell}$(Å)	I	$d_{hk\ell}$(Å)	I	$d_{hk\ell}$(Å)	I	$d_{hk\ell}$(Å)	hkℓ
200	7.602	10	7.62	31	7.42	21	7.41	10	7.414	100
002	6.954	8	6.96	5	6.84	17	6.79	7	6.835	002
$\bar{2}02$	5.388	---	5.39	4	---	---	---	---	5.267	$\bar{1}02$
202	4.908	13	4.905	2	4.821	16	4.815	18	4.815	$\bar{1}02$
$\bar{3}11$	4.518	13	4.517	<1	4.404	5	---	---	4.419	$\bar{1}11$
400	3.801	23	3.803	53	3.707	86	3.696	25	3.707	200
$\bar{3}11$	3.676	18	3.676	2	3.591	8	3.581	4	3.577	$\bar{2}11$
004	3.477	31	3.478	50	3.421	96	3.394	35	3.418	004
$\bar{4}02$	3.474	6			3.390	24	---	---	3.389	$\bar{2}02$
$\bar{3}13$	3.409	12	---	---	3.344	10	---	---	3.337	$\bar{1}13$
$\bar{2}04$	3.280	53	3.279	100	3.219	100	3.182	41	3.215	$\bar{1}04$
402	3.211	4	3.211	6	3.144	10	3.144	6	3.142	202
$\bar{2}22$	3.174	---	---	---	---	---	3.092	4	3.104	022
204	3.056	49	3.056	35	3.005	70	2.997	56	3.003	$\bar{1}04$
$\bar{5}11$	3.046	4	---	---	2.967	8	---	---	2.977	$\bar{2}11$
$\bar{4}20$	2.953	86	2.951	11	2.893	11	2.882	100	2.892	120
220	2.951	100			2.871	10	---	---	2.874	$\bar{2}20$
$\bar{2}22$	2.774	3	---	---	---	---	2.695	6	2.704	$\bar{2}22$
$\bar{4}04$	2.694	13	2.695	24	2.635	33	2.604	12	2.633	$\bar{2}04$
$\bar{1}15$	2.605	5	2.606	2	2.566	7	2.538	<1	2.556	015
$\bar{1}15$	2.573	8	2.574	2	2.519	7	---	---	2.525	$\bar{1}15$
600	2.534	15	2.535	35	2.470	70	2.463	15	2.471	300
$2\bar{2}4$	2.455	12	2.454	8	2.407	16	2.400	21	2.412	024
404	2.454	8							2.407	204
$\bar{6}20$	2.332	12	---	---	---	---	2.273	15	2.283	220
$3\bar{1}5$	2.319	---	2.319	9	2.278	12	---	---	2.281	115
006	2.318	1							2.278	006
602	2.312	3	2.313	12	2.261	8	---	---	2.260	302
$\bar{2}06$	2.277	31	2.278	49	2.236	84	2.213	25	2.235	$\bar{1}06$
224	2.190	4	---	---	---	---	2.145	7	2.141	$2\bar{2}4$
$6\bar{2}2$	2.166	17	---	---	2.125	6	2.116	29	2.125	$2\bar{2}2$
422	2.163	20	2.163	4	2.109	7	---	---	2.108	$3\bar{2}2$
$\bar{6}04$	2.145	5	2.145	6	2.093	11	2.071	6	2.094	$\bar{3}04$
$\bar{4}06$	2.067	3	2.066	10	2.024	10	2.000	4	2.024	$\bar{2}06$
$\bar{4}24$	2.005	5	---	---	---	---	1.941	6	1.956	$\bar{3}24$
604	1.962	8	1.962	5	1.922	10	1.921	10	1.922	$\bar{3}04$
$2\bar{2}6$	1.921	3	---	---	---	---	1.875	7	1.889	$1\bar{2}6$
800	1.900	3	1.900	12	1.853	10	1.846	4	1.853	400
$8\bar{2}0$	1.864	5	1.864	1	1.826	6	1.813	12	1.824	$3\bar{2}0$
620	1.864	4			1.814	6	---	---	1.813	$\bar{4}20$
$\bar{6}22$	1.838	4	1.837	1	---	---	---	---	1.789	$\bar{4}22$
$\bar{2}40$	1.816	33	---	---	---	---	1.776	16	1.774	$\bar{1}40$
$80\bar{2}$	1.791	3	1.791	6	1.750	11	1.746	4	1.750	402
$4\bar{2}6$	1.779	4	---	---	---	---	1,740	6	1.749	$12\bar{6}$
226	1.775	3							1.738	$2\bar{2}6$
008	1.738	19	1.739	18	1.708	44	1.697	16	1.709	008

Plus additional lines all with I ≤ 13

* Indices for the $\bar{P}\bar{1}$ unit cell and d (calc.) from the least-squares analysis of the Ca-bustamite X-ray powder data using the digital computer program of Appleman and Evans (1973). Calculated intensities from Borg and Smith (1969); data based on the structure determination of bustamite (54.5 mole% $CaSiO_3$) from Franklin, N.J., by Peacor and Buerger (1962).

** Indices for the $\bar{A}\bar{1}$ unit cell and d (calc.) from the least-squares analysis of the Mn-bustamite X-ray powder data.

† Ca-bustamite (78.8 mole% $CaSiO_3$) from Broken Hill, N.S.W., Australia (Mason, 1973). X-ray diffractometer conditions are: Chart No. X3900; Cu/Ni radiation; $\lambda CuK\alpha_1$=1.540598Å; Si used as internal standard; scanned at 1/4° per minute from 11-92° 2θ.

†† Mn-bustamite (33.8 mole% $CaSiO_3$) from Broken Hill, N.S.W., Australia (Mason, 1973). X-ray diffractometer conditions are: as above, except Chart No. X3894; scanned from 6-102° 2θ.

††† Santaclaraite heated in air at approximately 1,000°C for five hours. X-ray diffractometer conditions are: as above, except Chart No. X3902; scanned from 11-106° 2θ.

<anhydrous phase>	<hydrous phase>	
	add $2H_2O$	santaclaraite
M_5^{2+}	$M^{1+}M_4^{2+}H$	nambulite and marsturite
M_5^{2+}	$M^{3+}M_3^{2+}[]H$	babingtonite
M_{10}^{2+}	M_9^{2+} add $5H_2O$	inesite

where M represents octahedral cations and [] an unoccupied octadedral site. The reason that there are only nine (instead of ten) octahedra in inesite is related to the location of an inversion center. In inesite the inversion center is at the octahedral site M1 (the sequence is 5-4-3-2-1-2-3-4-5, thus nine in total), whereas in rhodonite it is between two M1 sites (*i.e.*, 5-4-3-2-1-1-2-3-4-5, thus ten in total).

The structural relations of these pyroxenoid minerals can be well understood in terms of different stacking schemes of tetrahedral and octadedral "building blocks", for which three types of hydrogen atoms, as H_2O, and O–

H · · · O, are responsible in the case of santaclaraite (Ohashi and Finger, 1981). The genetic relationships such as hydration and dehydration, however, are not known at present among the minerals listed in Table 4. When santaclaraite is heated, it does not transform to either $CaMn_4[Si_5O_{14}(OH)]$ or $CaMn_4[Si_5O_{15}]$, but the tetrahedral repeat length changes, as is discussed in the next section. Thus this relation for santaclaraite is another example of a phase change between pyroxenoids or pyroxenes with different tetradedral chain repeats (Morimoto *et al.*, 1966, for johannsenite–bustamite; Glasser and Glasser, 1961, for rhodonite–wollastonite; Aikawa, 1979, for rhodonite–pyroxmangite).

Dehydration to Mn-bustamite

We found early in our study that santaclaraite dehydrates in air at a low red heat to form Mn-bustamite. This reaction has been described at length by Ohashi and Finger (1981) and, although the mechanism is not discussed further here, it is of interest to compare the dehydration product with naturally occurring bustamite. Unit-cell (Table 5) and X-ray powder diffraction (Table 6) data are listed for dehydrated santaclaraite and for two bustamites from Broken Hill, N.S.W., Australia, that contain 78.8 and 33.8 mole percent $CaSiO_3$ and represent nearly limiting compositions of bustamite (Mason, 1975).

Agreement between the powder diffraction data of dehydrated santaclaraite and these two bustamites is excellent except for the intensity data. The X-ray diffractometer traces of Ca- and Mn-bustamite (Table 6) show a strong preferred orientation due to good cleavages on {100} and {001}. The strongest reflection in the calculated pattern (Borg and Smith, 1969) and in X-ray powder photographs prepared from a spherical mount is for *d* (220). The strongest line, without exception, for diffractometer traces is for *d* ($20\bar{4}$). This orientation effect is minimized in the pattern of the Mn-bustamite produced by heating santaclaraite as the transformation is not topotactic (Ohashi and Finger, 1981), and the observed intensities agree much better with those calculated from the crystal structure.

When the mole percentage of $CaSiO_3$ in naturally occurring bustamites is plotted against their molar volumes, the curve is seen to be essentially linear (Fig. 2). The slope of this line differs slightly from, but agrees reasonably well with, that given by Abrecht and Peters (1980, p. 265, Fig. 6). Extrapolation of this line suggests that the Mn-bustamite produced by dehydration of santaclaraite should contain about 24 mole percent $CaSiO_3$ for the molar volume observed. On the other hand, if the bulk composition of dehydrated santaclaraite (17.7 mole percent $CaSiO_3$) represents only Mn-bustamite, then the molar volume should be approximately 35.4 cm^3 or have a cell volume of about 705 $Å^3$. That such is not the case suggests that when santaclaraite is dehydrated by heating, it transforms chiefly to Mn-bustamite plus a minor amount of another phase or phases; these minor phases are either X-ray amorphous or insufficiently abundant to contribute to the X-ray diffraction pattern. In any case, the Mn-bustamite produced by heating santaclaraite above 550°C (Ohashi and Finger, 1981) must contain substantially less $CaSiO_3$ than the limiting mole ratio of 1/3 found for naturally occurring bustamite (Mason, 1975; Ohashi and Finger, 1978). Abrecht and Peters (1980), who have synthesized Mn-bustamite containing about 20 mole percent $CaSiO_3$, suggested that this result may indicate disorder in their synthetic high-temperature Mn-bustamite. However, a recent study by Yamanaka and Takéuchi (1981) has shown that a natural rhodonite with 18.10 mole percent $CaSiO_3$ could be transformed into bustamite. The plot of mole percent $CaSiO_3$ versus molar volume for their inverted bustamite plots very near to that of dehydrated santaclaraite in Figure 2.

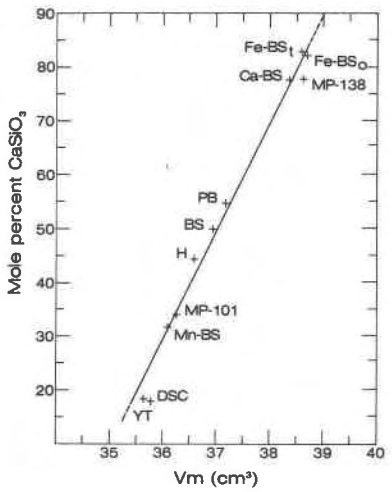

Fig. 2. Molar volume (*Vm*) *vs.* mole percentage of $CaSiO_3$ for bustamite and dehydrated santaclaraite. *Ferrobustamite*: Fe-BSt (Tsusue & Matsuoka, 1979), FeBSo (Yamanaka *et al.*, 1977). *Ca-bustamite*: MP-138 (Mason, 1973, molar volume determined in this study), Ca-BS (Ohashi & Finger, 1978). *Bustamite*: PB (Peacor & Buerger, 1962), BS (Ohashi & Finger, 1978), H (Harada *et al.*, 1974, volume recalculated). *Mn-bustamite*: MP-101 (Mason, 1973, molar volume determined in this study), Mn-BS (Ohashi & Finger, 1974), YT (Yamanaka & Takéuchi, 1981). *Dehydrated santaclaraite*: DSC (this study).

Acknowledgments

We thank Messrs. John L. Parnau and Albert L. McGuinness for the santaclaraite specimens and for furnishing us with a partial description of the discovery site. Permission to visit the Buckeye mine was granted us by Messrs. Rolland Seegers and Manuel Gonzales; specimens from the mine were provided by the late Dr. Max D. Crittenden, Jr. We are indebted to Dr. Brian H. Mason, of the Smithsonian Institution, Washington, D. C., for specimens of Ca- and Mn-bustamite from Broken Hill, N.S.W., Australia. This study was partly supported by National Science Foundation Grant EAR-77-15703. The manuscript bene-

fited from reviews by Drs. Judith A. Konnert, Eugene E. Foord, Peter Robinson, Howard W. Jaffe, and Donald R. Peacor.

References

Abrecht, J. and Peters, Tj. (1980) The miscibility gap between rhodonite and bustamite along the join $MnSiO_3$–$Ca_{0.60}Mn_{0.40}SiO_3$. Contributions to Mineralogy and Petrology, 74, 261–269.

Aikawa, N. (1979) Oriented intergrowth of rhodonite and pyroxmangite and their transformation mechanism. Mineralogical Journal (Japan), 9, 255–269.

Appleman, D. E. and Evans, H. T., Jr. (1973) Job 9214: Indexing and least squares refinement of powder diffraction data. U.S. Department of Commerce, National Technical Information Service Document PB-216188.

Araki, T. and Zoltai, T. (1972) Crystal structure of babingtonite. Zeitschrift für Kristallographie, 135, 355–373.

Bence, A. E. and Albee, A. L. (1968) Empirical correction factors for the electron microanalysis of silicates and oxides. Journal of Geology, 76, 382–403.

Borg, I. Y. and Smith, D. K. (1969) Calculated X-ray powder patterns for silicate minerals. Geological Society of America Memoir 122.

Davis, F. F. (1957) Manganese. In O. P. Jenkins and L. A. Wright, Eds., Mineral Commodities of California: California Division of Mines and Geology Bulletin 176, 325–339.

Deer, W. A., Howie, R. A., and Zussman, J. (1962) Rock-Forming Minerals, Vol. 5, Non-Silicates. Wiley, New York.

Finger, L. W. and Hadidiacos, C. G. (1972) Electron-microprobe automation. Carnegie Institution of Washington Year Book 71, 598–600.

Glasser, L. S. D. and Glasser, F. P. (1961) Silicate transformations: Rhodonite-wollastonite. Acta Crystallographica, 14, 818–822.

Harada, K., Sekino, H., Nagashima, K., Watanabe, T., and Momoi, H. (1974) High-iron bustamite and fluorapatite from the Broken Hill mine, New South Wales, Australia. Mineralogical Magazine, 39, 601–604.

Jenkins, O. P. Ed. (1943) Manganese in California. California Division of Mines and Geology Bulletin 125.

Mandarino, J. A. (1981) The Gladstone–Dale relationship: Part IV. The compatibility concept and its appliation. Canadian Mineralogist, 19, 441–450.

Mason, Brian (1973) Manganese silicate minerals from Broken Hill, New South Wales. Journal of the Geological Society of Australia, 20, Pt. 4, 397–404.

Mason, Brian (1975) Compositional limits of wollastonite and bustamite. American Mineralogist, 60, 209–212.

Morimoto, N., Koto, K., and Shinohara, T. (1966) Oriented transformation of johannsenite to bustamite. Mineralogical Journal (Japan), 5, 44–64.

Murakami, T., Takéuchi, Y., Tagai, T., and Koto, K. (1977) Lithium-hydrorhodonite. Acta Crystallographica, B33, 919–921.

Narita, H., Koto, K., and Morimoto, N. (1975) The crystal structure of nambulite $(Li,Na)Mn_4Si_5O_{14}(OH)$. Acta Crystallographica, B31, 2422–2426.

Ohashi, Y. and Erd, R. C. (1978) A new pyroxenoid $Mn_4CaSi_5O_{15} \cdot 2H_2O$: its structural relationship to rhodonite, nambulite and marsturite (abstr.). Geological Society of America Abstracts with Programs, 10, 465.

Ohashi, Y. and Finger, L. W. (1975) Pyroxenoids: a comparison of refined structures of natural rhodonite and pyroxmangite. Carnegie Institution of Washington Year Book 74, 564–569.

Ohashi, Y. and Finger L. W. (1978) The role of octahedral cations in pyroxenoid crystal chemistry. I. Bustamite, wollastonite, and the pectolite–schizolite, serandite series. American Mineralogist, 63, 274–288.

Ohashi, Y. and Finger, L. W. (1981) The crystal structure of santaclaraite, $CaMn_4[Si_5O_{14}(OH)](OH) \cdot H_2O$: the role of hydrogen atoms in the pyroxenoid structure. American Mineralogist, 66, 154–168.

Peacor, D. R. and Buerger, M. J. (1962) Determination and refinement of the crystal structure of bustamite, $CaMnSi_2O_6$. Zeitschrift für Kristallographie, 117, 331–343.

Peacor, D. R. and Niizeki, N. (1963) The redetermination and refinement of the crystal structure of rhodonite, $(Mn,Ca)SiO_3$. Zeitschrift für Kristallographie, 119, 98–116.

Peacor, D. R., Dunn, P., and Sturman, B. D. (1978) Marsturite, $Mn_3CaNaHSi_5O_{15}$, a new mineral of the nambulite group from Franklin, New Jersey. American Mineralogist, 63, 1187–1189.

Smith, D. K. and Holomany, M. (1978) A FORTRAN IV program for calculating X-ray powder diffraction patterns—Version 7. The Pennsylvania State University, University Park, Pennsylvania, p. 1–63.

Trask, P. D. Ed. (1950) Geologic description of the manganese deposits of California. California Division of Mines and Geology Bulletin 152.

Tsusue, A. and Matsuoka, M. (1979) Ferrobustamite from the Tsumo mine, Shimane Prefecture, Japan. Kumamoto Journal of Science, Geology, ll, 1–9.

Wan, C. and Ghose, S. (1978) Inesite, a hydrated calcium manganese silicate with five-tetrahedral-repeat double chains. American Mineralogist, 63, 563–571.

Yamanaka, T. and Takéuchi, Y. (1981) X-ray study of the rhodonite-bustamite transformation. Zeitschrift für Kristallographie, 157, 131–145.

Yamanaka, T., Sadanaga, R., and Takéuchi, Y. (1977) Structural variation in the ferrobustamite solid solution. American Mineralogist, 62, 1216–1224.

Manuscript received, June 30, 1982;
accepted for publication, May 25, 1983.